PCCP

Linear free-energy relationship for electron-transfer processes of pyrrolidinofullerenes with tetrakis(dimethylamino)ethylene in ground and excited states

Chuping Luo,*[a] Mamoru Fujitsuka,[a] Chun-Hui Huang[b] and Osamu Ito*[a]

[a] *Institute for Chemical Reaction Science, Tohoku University, Katahira, Aoba-ku, Sendai 980-8577, Japan*
[b] *State Key Laboratory of Rare Earth Materials Chemistry and Applications, Peking University, Beijing 100871, China*

Received 9th March 1999, Accepted 27th April 1999

Systematic studies of electron-transfer processes in the ground states and excited triplet states of pyrrolidinofullerenes $\{C_{60}(C_3H_6N)R\ [R = H$ (**1**), p-$C_6H_4NO_2$ (**2**), p-C_6H_4CHO (**3**), p-C_6H_5 (**4**), p-C_6H_4OMe (**5**), p-$C_6H_4NMe_2$ (**6**)$]\}$ with tetrakis(dimethylamino)ethylene (TDAE) have been carried out by steady-state and transient absorption measurements in the visible–NIR region. Analyses of the equilibria of the electron-transfer processes in the ground states indicate that free ion radicals are produced in polar solvents. Photoinduced electron-transfer processes *via* $^{T}(C_{60}(C_3H_6N)R)^*$ were observed by applying a perturbation to the equilibria of the electron-transfer reactions in the ground states by laser flash photolysis. Based on the relationship of the thermodynamic data and kinetic data, the electron-transfer rate constants in the ground states (k_{et}^{G}) can be evaluated. The k_{et}^{G} values are affected by the substituents to a smaller extent compared with the equilibrium constants (K) in polar solvents; $\alpha = 0.6$ in $\Delta \log k_{et}^{G} = \alpha\, \Delta \log K$. This α value indicates that the activation energies of forward electron transfer in the ground states vary moderately with the thermodynamic stabilities of $(C_{60}(C_3H_6N)R)^{\bullet -}$. Electron-transfer rate constants *via* $^{T}(C_{60}(C_3H_6N)R)^*$, which are close to the diffusion-controlled limit, do not show a large substituent effect ($\alpha' = 0$), because of their highly exothermic processes. Such a linear free-energy relationship can be extended to other systems such as $^{T}(C_{60}(C_3H_6N)R)^*$/*N*,*N*-dimethylaniline, from which valuable information for electron-transfer processes can be obtained.

Introduction

The high electron-accepting ability of fullerenes has played a significant role in fullerene chemistry, which relates to the studies of functionalization,[1] photocurrent generation,[2] superconductivity,[3] ferromagnetism[4] and various topics in biological applications.[5] The electrochemical studies pointed out that the functionalized fullerenes still keep electron-acceptor ability.[6] Thus, some C_{60} dyads connected with donors such as dimethylaniline,[7] ferrocene,[8] porphyrin[9] and carotenoid[10] have been studied on purpose to establish the efficient photoinduced charge-separation systems and to mimic photosynthetic reaction centers. It is also reported that intermolecular electron-transfer processes are decelerated by the functionalized groups[11] and affected by the site and degree of functionalization,[12] which can be rationalized in terms of perturbation on the π-system of fullerenes.

It is well known that tetrakis(dimethylamino)ethylene (TDAE) with a high oxidation potential ($E_{ox} = -0.75$ V *vs.* SCE in acetonitrile)[13] forms an ion radical salt with C_{60}, which shows ferromagnetism at low temperature.[4a] In C_{60}/TDAE solutions, reversible electron transfer takes place in both ground state and excited triplet state as reported in our previous paper.[14]

In the present work, the electron-transfer processes of pyrrolidinofullerenes (Scheme 1) with TDAE were systematically studied. By steady-state visible–NIR absorption spectra, the equilibrium constants of electron transfer between TDAE and $C_{60}(C_3H_6N)R$ in the ground state were measurable; it is expected that the free ion radicals are formed in highly polar solvents. Photoinduced electron-transfer processes can also be observed by laser flash photolysis, which causes a perturbation of the equilibria in the ground state. Considering these thermodynamic and kinetic data, the electron-transfer rate constants in the ground state can be evaluated. We obtained both equilibrium and kinetic data; thus, the linear free-energy relationship (LFER) can be used to explain the substituent effect on the electron-transfer processes. Based on the coefficients of the LFER, the substituent effects observed on the forward and backward electron-transfer processes can be explained by the potential energy curves.

Experimental

Materials

Pyrrolidinofullerenes were synthesized as reported in our previous paper.[2c] C_{60}(>99.9%) was purchased from Texas Fullerenes Corp. Tetrakis(dimethylamino)ethylene (TDAE) was of commercially available best grade. Solvents were of spectroscopic or HPLC grade.

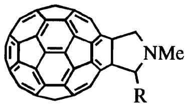

R= H (**1**), p-$C_6H_4NO_2$ (**2**), p-C_6H_4CHO (**3**), p-C_6H_5 (**4**), p-C_6H_4OMe (**5**), p-$C_6H_4NMe_2$ (**6**)

Scheme 1

Measurements

All measurements were carried out in the dark by using a quartz cell (1 cm) under an Ar atmosphere at room temperature. Steady-state absorption spectra in the visible–NIR region were measured on a JASCO/V-570 spectrometer. EPR spectra were measured on a Varian E-4. Transient absorption spectra in the NIR region were measured by means of laser flash photolysis; 532 nm light from a Nd:YAG laser was used as the exciting source and a Ge avalanche photodiode module was used for detecting the monitoring light from a pulsed Xe lamp as described in our previous report.[15]

Results and discussion

Electron transfer in the ground state

On addition of TDAE to a benzonitrile/toluene (BN/Tol, v/v 1 : 1) solution of $C_{60}(C_3H_6N)R$ at room temperature, new broad absorption bands appear in the NIR region with $\lambda_{max} \approx 1000$ nm (Fig. 1), which are attributed to the absorption bands of the anion radicals of pyrrolidinofullerenes ($(C_{60}(C_3H_6N)R)^{\bullet -}$) by the similarity to the band of $C_{60}^{\bullet -}$.[11d,16] Therefore, the electron-transfer reactions take place in ground states. Since the shape and the position of the absorption bands did not change appreciably on addition of excess TDAE, one-electron transfer takes place predominantly, indicating that dianions are not produced by two-electron transfer.[17] As the absorption intensities of $(C_{60}(C_3H_6N)R)^{\bullet -}$ increase with the concentration of TDAE (Fig. 1), thermal equilibria exist for these electron-transfer processes as represented in eqn. (1) ($R' = (C_3H_6N)R$), in which the free ion radicals are assumed to be produced in polar solvent after electron transfer takes place:

$$C_{60}R' + \text{TDAE} \underset{k_{\text{bet}}^{\text{G}}}{\overset{k_{\text{et}}^{\text{G}}}{\rightleftharpoons}} (C_{60}R')^{\bullet -} + \text{TDAE}^{+\bullet} \tag{1}$$

In eqn. (1), the equilibrium constants can be defined as $K_2 = k_{\text{et}}^{\text{G}}/k_{\text{bet}}^{\text{G}}$, where suffix 2 implies that the backward electron reactions are bimolecular processes. Then, eqn. (2) can be derived with the assumption that the concentrations of the ion radicals are negligible as compared with the initial concentration of TDAE ($[\text{TDAE}]_0$):

$$\frac{[\text{TDAE}]_0}{\text{Abs}} = \frac{[C_{60}R']_0[\text{TDAE}]_0}{(\text{Abs})^2}\,\varepsilon - \frac{1}{K_2\,\varepsilon} \tag{2}$$

where $[C_{60}R']_0$ refers to the initial concentration of $C_{60}(C_3H_6N)R$; Abs and ε are the absorbance and molar absorption coefficients of $(C_{60}(C_3H_6N)R)^{\bullet -}$ at their maximal peak wavelength, respectively. From eqn. (2), the values of K_2 and ε in BN/Tol were evaluated as summarized in Table 1. In comparison with the K_2 value of C_{60}, the K_2 values of $C_{60}(C_3H_6N)R$ are smaller by factors of 1/50 to 1/240, indicating that the electron-accepting ability of the C_{60} moiety decreases after functionalization. The K_2 values of **2** and **3** with electron-withdrawing groups are *ca.* 4 times larger than those of other derivatives, suggesting that the electron-withdrawing groups cause a decrease of the electron density on the skeleton of the fullerene moiety and result in a recovery of the electron-accepting ability.

Taking K_2 values into consideration, net absorption spectra of $(C_{60}(C_3H_6N)R)^{\bullet -}/\text{TDAE}^{+\bullet}$ can be obtained by subtracting the absorption spectra of $C_{60}(C_3H_6N)R$ and TDAE (Fig. 2). The ε values of $(C_{60}(C_3H_6N)R)^{\bullet -}$ at *ca.* 1000 nm are smaller than that of $C_{60}^{\bullet -}$ at 1070 nm; λ_{max} shifts to shorter wavelength with the broadening of each peak, which may result

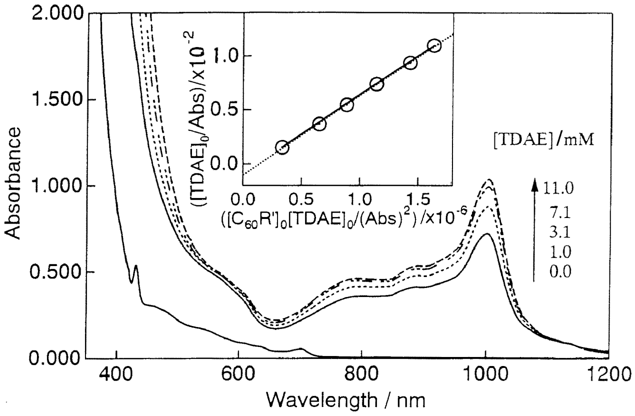

Fig. 1 Steady-state absorption of $C_{60}((C_3H_6N)(C_6H_4NO_2))$ (0.15 mM) with changing concentration of TDAE in argon bubbled benzonitrile/toluene (v/v 1 : 1) solution at room temperature (optical length: 1 cm). Insert: Plot according to eqn. (2) ($R' = (C_3H_6N)R$).

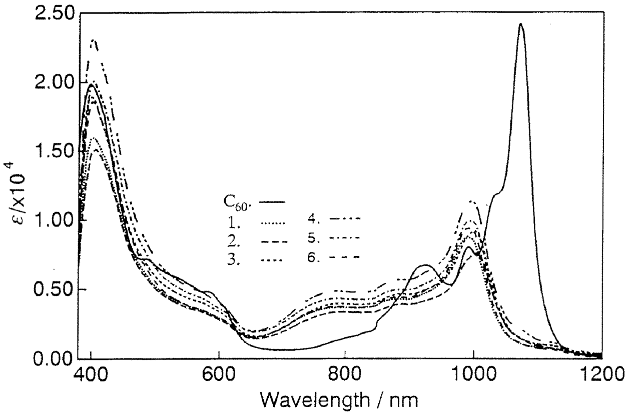

Fig. 2 Absorption spectra of $C_{60}^{\bullet -}/\text{TDAE}^{+\bullet}$ and $(C_{60}(C_3H_6N)R)^{\bullet -}/\text{TDAE}^{+\bullet}$ in argon bubbled benzonitrile/toluene (v/v 1 : 1) solution at room temperature obtained by subtracting the spectra of TDAE and C_{60} or $C_{60}(C_3H_6N)R$ from the total ones.

Table 1 Absorption maxima (λ_{max}) and molar absorption coefficients (ε_{max}) of $C_{60}^{\bullet -}$ and $C_{60}(C_3H_6N)^{\bullet -}$ and equilibrium constants (K_2 and K_1) of C_{60} and $C_{60}(C_3H_6N)R$ with TDAE[a]

	C_{60}	H **1**	$C_6H_4NO_2$ **2**	C_6H_4CHO **3**	Ph **4**	C_6H_4OMe **5**	$C_6H_4NMe_2$ **6**
In BN/Tol:							
λ_{max}/nm	1072	991	1002	1000	995	994	990
$K_2/10^{-2}$	634	3.63	13.5	11.2	2.65	2.93	4.53
$\varepsilon_{max}/10^3$ mol^{-1} dm^3 cm^{-1}	23.9	8.41	7.31	8.85	8.61	9.53	9.23
In CB:							
λ_{max}/nm	1073	990	1003	999	1000	994	994
K_1/M^{-1}	40	6	16	13	7	9	10
$\varepsilon_{max}/10^3$ mol^{-1} dm^3 cm^{-1}	9.7	0.47	0.88	0.73	0.88	0.43	0.44

[a] Estimation error: λ_{max} (±0.1 nm), K_2 (±5%), ε_{max} (±5%), and K_1 (±7%).

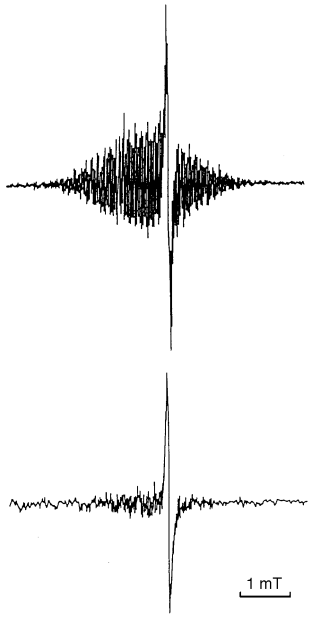

Fig. 3 EPR spectra of $C_{60}((C_3H_6N)(C_6H_4NO_2))$ with TDAE in BN/Tol (top) and in CB (bottom) at room temperature.

from the change of π-electron distribution on the spherical skeleton of C_{60}, probably caused by the reduction of molecular symmetry after functionalization. Among these derivatives, the λ_{max} values for the derivatives with the electron-withdrawing groups obviously shift to longer wavelength than those with the electron-donating groups; *i.e.*, λ_{max} of $\mathbf{2}^{\bullet -}$ with NO_2 shifts 10 nm as compared with that of $\mathbf{6}^{\bullet -}$ with NMe_2. The maximal shift of λ_{max} among these anion radicals (121 cm^{-1}) is the same as that among the neutral molecules as reported previously.[18]

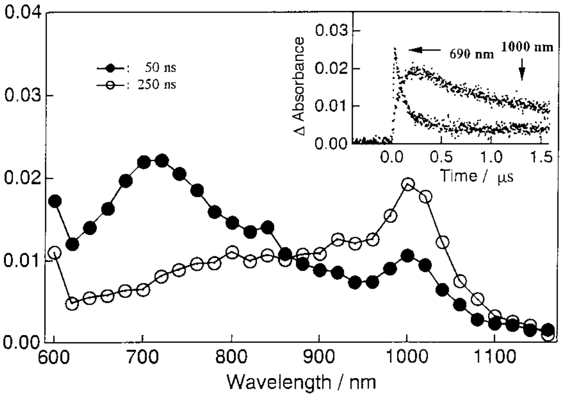

Fig. 4 Transient absorption spectra of $C_{60}((C_3H_6N)(C_6H_4NO_2))$ (0.16 mM) with TDAE (1.38 mM) in BN/Tol. Insert: Decay at 690 nm and rise at 1000 nm.

In less polar chlorobenzene (CB), the equilibrium data do not obey eqn. (2), although the absorption spectral shapes and λ_{max} values of $(C_{60}(C_3H_6N)R)^{\bullet -}$ are similar to those in BN/Tol. It is assumed that the ion radicals are present as ion pairs in the less polar solvent [eqn. (3)]:

$$C_{60}R' + \mathrm{TDAE} \underset{k_{bet}^{G}}{\overset{k_{et}^{G}}{\rightleftharpoons}} [(C_{60}R')^{-\bullet}, \mathrm{TDAE}^{+\bullet}] \qquad (3)$$

Then, K_1 is defined as k_{et}^G/k_{bet}^G, in which k_{bet}^G is the first-order process, but not the second-order process as eqn. (1). The K_1 and ε values were evaluated by the Benesi–Hildebrand equation:[19]

$$\frac{[C_{60}R']_0}{\mathrm{Abs}} = \frac{1}{K_1\varepsilon}\,\frac{1}{[\mathrm{TDAE}]_0} + \frac{1}{\varepsilon} \qquad (4)$$

The ε_{max} values evaluated by the Benesi–Hildebrand plots in CB are somewhat smaller than those in BN/Tol (Table 1), suggesting that some extra reactions may occur in addition to a reversible electron-transfer process. Therefore, one must be careful in using these ε_{max} values; in the present study, we did not employ these values for further study.

The formation of the ion radicals can be detected by EPR as shown in Fig. 3. In BN/Tol, the EPR spectrum consists of hyperfine structures and a narrow signal [Fig. 3(a)]. The hyperfine splitting is well simulated by the reported values for $\mathrm{TDAE}^{+\bullet}$.[14] The narrow signal at $g = 2.0002$ to $(C_{60}(C_3H_6N)R)^{\bullet -}$ is very close to those of the anion radicals of other C_{60} derivatives.[20] Such sharp lines may indicate that $\mathrm{TDAE}^{+\bullet}$ and $(C_{60}(C_3H_6N)R)^{\bullet -}$ are present as free ion radicals in BN/Tol. In CB, only a narrow line signal of $(C_{60}(C_3H_6N)R)^{\bullet -}$ was observed [Fig. 3(b)], suggesting that some reactions occur for $\mathrm{TDAE}^{+\bullet}$; degradation and/or dimerization of $\mathrm{TDAE}^{+\bullet}$ may be considered as reasons for the disappearance of the EPR signals of $\mathrm{TDAE}^{+\bullet}$. This may be related to difficulties in the analyses of the equilibrium data in CB.

Electron transfer *via* $^{T}(C_{60}(C_3H_6N)R)^*$

By 532 nm laser irradiation, which predominantly excites $(C_{60}(C_3H_6N)R)$, the thermal equilibria of the electron-transfer processes in the ground state are perturbed. The neutral $C_{60}(C_3H_6N)R$ in eqn. (1) can be excited to the singlet state, which decays to the triplet states ($^{T}(C_{60}(C_3H_6N)R)^*$) by intersystem crossing. Fig. 4 shows the transient absorption spectra of **2** in the presence of excess TDAE in BN/Tol; the baseline of absorbance (Abs = 0) is set at the absorbance of the

Table 2 Electron-transfer rate constants and back electron-transfer rate constants of C_{60} and $C_{60}(C_3H_6N)R$ with TDAE in the ground and excited triplet states[a]

	C_{60}	H **1**	$C_6H_4NO_2$ **2**	C_6H_4CHO **3**	Ph **4**	C_6H_4OMe **5**	$C_6H_4NMe_2$ **6**
In BN/Tol:							
k_{et}^{T} [b]$/10^9$ mol^{-1} dm^3 s^{-1}	–[c]	7.2	11	9.8	12	9.1	8.5
$k_{bet}^{2nd}/10^{10}$ mol^{-1} dm^3 s^{-1}	–[c]	2.0	1.1	0.99	2.0	2.0	2.3
$k_{et}^{G}/10^8$ mol^{-1} dm^3 s^{-1}	–[c]	7.2	15	11	5.3	5.9	10
In CB:							
k_{et}^{T} [b]$/10^9$ mol^{-1} dm^3 s^{-1}	3.3	8.6	8.3	6.5	8.4	5.8	7.9
$k_{bet}^{1st}/10^7$ s^{-1}	1.2	0.26	0.35	0.29	0.26	0.29	0.28
$k_{et}^{G}/10^7$ mol^{-1} dm^3 s^{-1}	48	(1.6)	(5.6)	(3.8)	(1.8)	(2.6)	(2.8)

[a] Estimation error: k_{et}^{T} (±5%), k_{bet}^{2nd} (±7%), k_{bet}^{1st}(±5%), and k_{et}^{G} (±10%). [b] Φ_{et} values of $C_{60}(C_3H_6N)R$ in BN/Tol and CB were asssumed to be unity. [c] Electron transfer *via* $^{T}C_{60}^*$ cannot be observed, because of the large equilibrium constants.

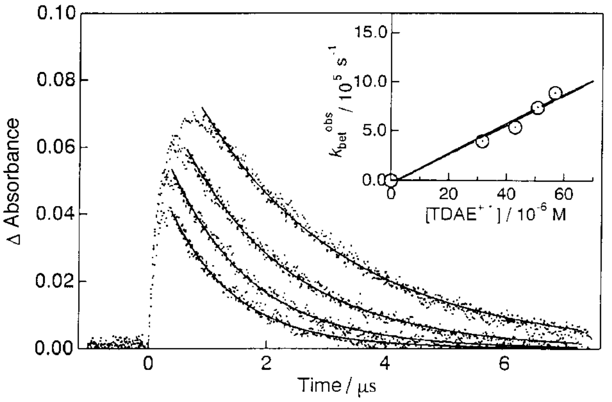

Fig. 5 Long time-scale profile of $(C_{60}((C_3H_6N)(C_6H_4NO_2)))^{-\bullet}$ in BN/Tol. Insert: $k_{\rm bet}^{\rm obs}$ *vs.* $[TDAE^{+\bullet}]$.

thermal equilibrium components at each wavelength. The absorption band appearing at 690 nm is due to $^T(C_{60}(C_3H_6N)R)^*$.[18] With the decay of $^T(C_{60}(C_3H_6N)R)^*$, the absorption band at 1000 nm increases, which can be assigned to $(C_{60}(C_3H_6N)R)^{\bullet-}$ based on the steady-state absorption spectrum. The mirror image of the decay time profile of $^T(C_{60}(C_3H_6N)R)^*$ with the rise time profile of $(C_{60}(C_3H_6N)R)^{\bullet-}$ suggests that the electron-transfer processes take place from neutral TDAE to $^T(C_{60}(C_3H_6N)R)^*$ after the laser pulse. The electron-transfer processes can be represented as eqn. (5), in which $\{(C_{60}R')^{\bullet-}\}_{h\nu}$ and $\{TDAE^{+\bullet}\}_{h\nu}$ are the ion radicals produced by laser exposure of $(C_{60}(C_3H_6N)R)$ in addition to the ion radicals present at thermal equilibrium, $\{(C_{60}R')^{\bullet-}\}_{\rm eq}$ and $\{TDAE^{+\bullet}\}_{\rm eq}$, before laser exposure:

$$^T(C_{60}R')^* + \{TDAE\}_{\rm eq} \xrightarrow[\Phi_{\rm et}]{k_{\rm et}^{\rm T}} \{(C_{60}R')^{\bullet-}\}_{h\nu} + \{TDAE^{+\bullet}\}_{h\nu} \tag{5}$$

From the ratios of the maximal concentrations of $\{(C_{60}(C_3H_6N)R)^{\bullet-}\}_{h\nu}$ to those of $^T(C_{60}(C_3H_6N)R)^*$, the quantum yields of electron transfer ($\Phi_{\rm et}$) were evaluated as unity in BN/Tol, indicating that $^T(C_{60}(C_3H_6N)R)^*$ are predominantly consumed by the electron-transfer processes.

The decay profiles of $^T(C_{60}(C_3H_6N)R)^*$ obey first-order kinetics under the pseudo-first-order condition, *i.e.* the equilibrium concentration of TDAE ($[TDAE]_{\rm eq}$) is far in excess of $^T(C_{60}(C_3H_6N)R)^*$ produced by a laser exposure. The second-order electron-transfer rate constants (k_q) can be obtained from the slopes by pseudo-first-order plots with respect to $[TDAE]_{\rm eq}$. On considering $\Phi_{\rm et} = 1$, the rate constants of electron transfer ($k_{\rm et}^{\rm T}$) *via* $^T(C_{60}(C_3H_6N)R)^*$ were evaluated by the relation $k_{\rm et}^{\rm T} = k_q$ as summarized in Table 2. In less polar CB, the $k_{\rm et}^{\rm T}$ values were estimated by assuming $\Phi_{\rm et} = 1$, because reliable $\varepsilon_{\rm max}$ values were not obtained. All $k_{\rm et}^{\rm T}$ values are almost the same and close to the diffusion-controlled limit ($k_{\rm diff}$). The substituent effect on $k_{\rm et}^{\rm T}$ is smaller than that on K_2. The small substituent effect on $k_{\rm et}^{\rm T}$ indicates that electron transfer *via* $^T(C_{60}(C_3H_6N)R)^*$ is highly exothermic for all reactions.

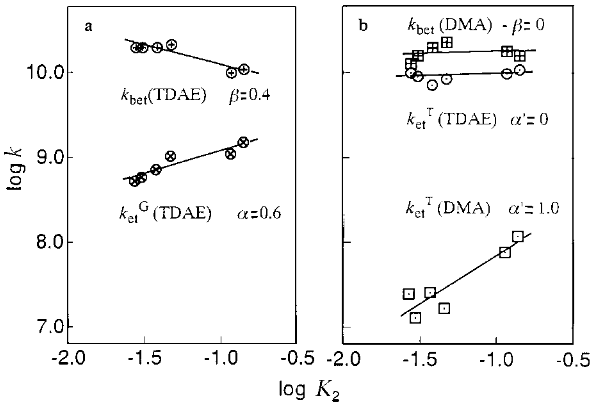

Fig. 6 Linear free-energy relationship for electron-transfer processes of $C_{60}(C_3H_6N)R$ with TDAE in ground (a) and triplet (b) states and with DMA in triplet state (b) in BN/Tol solution.

Estimation of $k_{\rm bet}$

After reaching the maxima, the absorption intensities of $\{(C_{60}(C_3H_6N)R)^{\bullet-}\}_{h\nu}$ in BN/Tol begin to decay gradually as shown in Fig. 5. Each decay curve obeys first-order kinetics, since large excesses of $[TDAE^{+\bullet}]_{\rm total}$ ($= [TDAE^{+\bullet}]_{\rm eq} + [TDAE^{+\bullet}]_{h\nu}$, *ca.* 0.098 mM) are present with respect to $[(C_{60}(C_3H_6N)R)^{\bullet-}]_{h\nu}$ (*ca.* 0.008 mM) as calculated by using K_2 in Table 1. Then, the back electron-transfer rate constants ($k_{\rm bet}^{\rm 2nd}$) for eqn. (6) were evaluated from the slopes of the linear relation of the plots of the first-order rate constants *vs.* $[TDAE^{+\bullet}]_{\rm eq}$ ($\gg [TDAE^{+\bullet}]_{h\nu}$) as shown in the insert in Fig. 5:

$$\{(C_{60}R')^{\bullet-}\}_{h\nu} + \{TDAE^{+\bullet}\}_{h\nu} \xrightarrow[{[(C_{60}R)^{\bullet-}]_{\rm eq},\ [TDAE^{+\bullet}]_{\rm eq}}]{k_{\rm bet}^{\rm 2nd}} C_{60}R' + TDAE \tag{6}$$

In the less polar CB, the decays of $\{(C_{60}(C_3H_6N)R)^{\bullet-}\}_{h\nu}$ also obey first-order kinetics; however, the decay rates were not increased by the concentration of $[TDAE^{+\bullet}]_{\rm total}$, suggesting that the decays are of monomolecular kinetics. Such behavior would be anticipated, when the contact ion pairs are predominantly formed and the back electron transfer takes place within the ion pairs. The $k_{\rm bet}^{\rm 1st}$ values were evaluated as listed in Table 2.

In CB, the decay of $\{C_{60}^{\bullet-}\}_{h\nu}$ was as fast as the decay of $^TC_{60}^*$; the decay of $\{C_{60}^{\bullet-}\}_{h\nu}$ seems to be influenced by the decay of $^TC_{60}^*$, which is also supported by the fact that the decay rate of $\{C_{60}^{\bullet-}\}_{h\nu}$ increases with the addition of [TDAE]. These results imply that the ion pair between $\{C_{60}^{\bullet-}\}_{h\nu}$ and $\{TDAE^{+\bullet}\}_{h\nu}$ is quite strong in less polar solvents such as CB. In Table 2, the maximal $k_{\rm bet}^{\rm 1st}$ value is listed. In the cases of the derivatives, such dependence may not occur, because the ion pairs between $\{(C_{60}(C_3H_6N)R)^{\bullet-}\}_{h\nu}$ and $\{TDAE^{+\bullet}\}_{h\nu}$ are not as strong as that between $\{C_{60}^{\bullet-}\}_{h\nu}$ and $\{TDAE^{+\bullet}\}_{h\nu}$, probably due to the steric effect of the substituents.

Evaluation of $k_{\rm et}^{\rm G}$

Based on kinetic and equilibrium data evaluated above, the electron-transfer rate constants in the ground states ($k_{\rm et}^{\rm G}$) in BN/Tol can be calculated by the relation $k_{\rm et}^{\rm G} = K_2 k_{\rm bet}^{\rm 2nd}$, where $k_{\rm bet}^{\rm 2nd} = k_{\rm bet}^{\rm G}$. All the calculated data are listed in Table 2, from which it is obvious that the introduced substituent considerably influences the $k_{\rm et}^{\rm G}$ values. In the case of less polar solvents, $k_{\rm et}^{\rm G}$ also can be obtained from $K_1 k_{\rm bet}^{\rm 1st}$, but K_1 may contain some ambiguity. Then, the $k_{\rm et}^{\rm G}$ values in these solvents are listed in parentheses.

Linear free-energy relationship

The substituent effect on kinetic data can be expressed by the linear free-energy relationship (LFER) on the basis of the substituent effect on the equilibrium constants as eqns. (7) and (8):[21]

$$\Delta \log k_{\rm et}^{\rm G} = \alpha\, \Delta \log K \tag{7}$$

$$\Delta \log k_{\rm bet}^{\rm G} = -\beta\, \Delta \log K \tag{8}$$

The plots of log k_{et}^{G} and log k_{bet}^{G} *vs.* logK_2 in BN/Tol are shown in Fig. 6(a); the significant substituent effect on the forward electron-transfer processes in the ground state is apparent with a steeper slope. The slopes yield α and β; $\alpha = 0.6$ and $\beta = 0.4$ [Fig. 6(a)]. The observation $\alpha > \beta$ implies that the forward electron-transfer processes demand considerable activation energies, which vary with the difference in thermodynamic stabilities of the products (ion radicals) and reactants (neutral molecules). On the other hand, the backward electron-transfer processes are less dependent on the K_2 values.

In less polar solvents such as CB, α and β are 1.0 and 0, respectively, although the K_1 values may contain some ambiguity. These slopes indicate that the forward electron-transfer processes become more dependent on the K values, which implies that the forward electron-transfer processes become endothermic with a decrease in the solvent polarity.

In the case of k_{et}^{T} [Fig. 6(b)] in BN/Tol, the k_{et}^{T} values are not remarkably changed with the K_2 values (slope = 0). This indicates that the electron-transfer reactions *via* the triplet state are quite exothermic; thus, the k_{et}^{T} values are all close to the diffusion-controlled limit.

The Δ log K_2 values for TDAE can be applied to other donor systems in the same solvent systems. For example, the k_{et}^{T} values for the electron-transfer reactions between $^{T}(C_{60}(C_3H_6N)R)^*$ and *N*,*N*-dimethylaniline (DMA) in BN/Tol[11d] are plotted against the K_2values for TDAE [Fig. 6(b)]. The slopes of $\alpha' = 1$ ($\Delta \log k_{et}^{G} = \alpha' \, \Delta \log K_2$) and $\beta = 0$ [eqn. (8)] suggest that the activation energies for the forward electron-transfer processes are higher, while those of the backward processes are quite low. These facts suggest that the substituent effect on forward electron-transfer processes *via* $^{T}(C_{60}(C_3H_6N)R)^*$ becomes larger on decreasing the electron-donating ability of donors.

The relationship can be explained by the energy diagram (Fig. 7), in which the free-energy changes (ΔG_{et}) of the electron-transfer processes were calculated by the Rehm–Weller relation.[11d,23] Based on this relation, the ΔG_{et}^{T} value *via* $^{T}(C_{60}(C_3H_6N)R)^*$ is *ca.* −40 kcal mol^{-1} in BN/Tol, which confirms the high exothermicity of electron transfer *via* $^{T}(C_{60}(C_3H_6N)R)^*$. Thus, in the potential curves shown in Fig. 7(a), the line of the free ion radicals crosses at the minimum valley of $^{T}(C_{60}(C_3H_6N)R)^*$, yielding a negligible activation energy for k_{et}^{T}. In the ground state, slightly positive ΔG_{et}^{G} (*ca.* −6 kcal mol^{-1}) was obtained in BN/Tol, indicating that the forward electron-transfer process is slightly exothermic. Both forward and backward electron-transfer processes need considerable activation energy [Fig. 7(a)] as assumed by the observed α and β values.

In less polar solvents such as CB, on the other hand, the ΔG_{et}^{G} value might be slightly positive because of the small k_{et}^{G} values (10^7–10^8 M^{-1} s^{-1}). Therefore, the potential curve of neutral molecules in the ground state crosses near the minimum of the potential curve of the ion radicals, suggesting that the activation energies of the back electron-transfer processes are quite small [Fig. 7(b)], which is consistent with $\beta = 0$. From the potential curves in Fig. 7(b), $\alpha = 1$ is satisfied. A tendency of $k_{et}^{T} > k_{et}^{G}$ can also be explained by this potential energy diagram.

For the electron-transfer processes *via* $^{T}(C_{60}(C_3H_6N)R)^*$ with DMA in BN/Tol, the potential curve of neutral molecules in the ground state crosses the minimum of the potential curve of the ion radicals [Fig. 7(c)]. Then, back electron-transfer processes are very fast, while the forward electron-transfer processes strongly depend on the substituents.

Conclusion

Substituent effects on the electron-transfer processes between pyrrolidinofullerenes and TDAE were studied in both ground state and excited triplet state. Complete sets of equilibrium constants and rate constants for forward and backward electron-transfer processes in the ground state were obtained in solvents with different polarities, in addition to the rate constants of forward electron transfer in the excited triplet state. Thus, the linear free-energy relationship was invoked to explain the electron-transfer processes, from which the origin of the observed substituent effects on the electron-transfer rates can be clarified, including a change of the solvent polarity. From these considerations, the potential energy diagrams for the electron-transfer processes in both ground and triplet states can be unequivocally illustrated.

Acknowledgements

The authors would like to thank Dr. A. Watanabe (Tohoku University) for his assistance in spectroscopic measurements and Dr. L. Gan and Mr. Y. Huang (Peking University) for sample preparations. The present work was partly supported

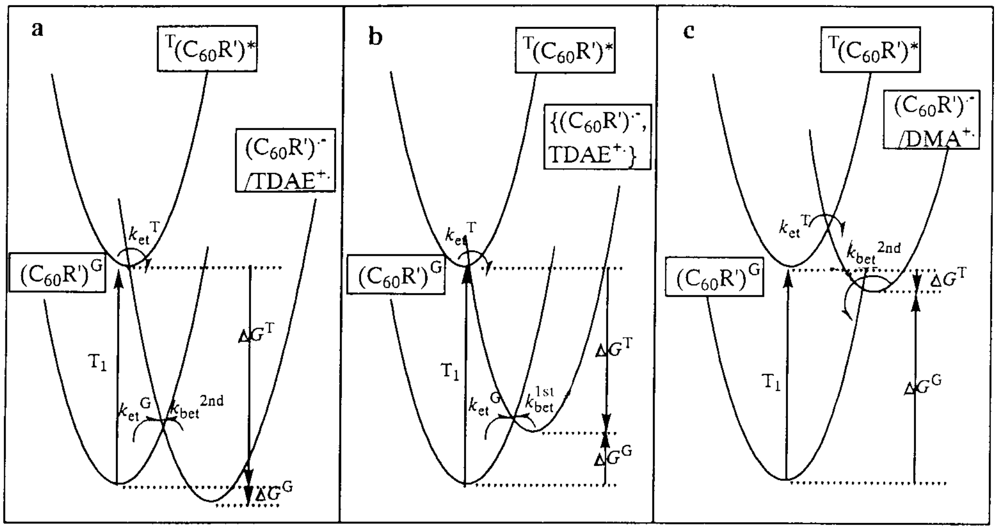

Fig. 7 Energy diagram of electron-transfer processes of $C_{60}R'$($R' = (C_3H_6N)R$) with TDAE in BN/Tol (a) and CB (b) and with DMA in BN/Tol (c).

by the Grant-in-Aid on Priority-Area-Research on "Laser Chemistry of Single Nanometer Organic Particle" (No. 10207202) and on "Carbon Alloys" (No. 10137203) from the Ministry of Education, Science, Sports and Culture of Japan.

References

1 (*a*) T. Suzuki, Q. Li, K. C. Khemani, F. Wudl and Ö. Almarsson, *Science*, 1991, **254**, 1186; (*b*) F. Wudl, *Acc. Chem. Res.*, 1992, **25**, 157; (*c*) A. Hirsch, A. Soi and H. R. Karfunkel, *Angew. Chem., Int. Ed. Engl.*, 1992, **31**, 766; (*d*) C. Bingel, *Chem. Res.*, 1993, **126**, 1957; (*e*) J. M. Hawkins, M. Nambu and A. Meyer, *J. Am. Chem. Soc.*, 1994, **116**, 7642; (*f*) S. R. Wilson, Q. Lu, J. Cao, Y. Wu, C. J. Welch and D. I. Schuster, *Tetrahedron*, 1996, **52**, 5131; (*g*) J-N. Nierengarten, T. Habicher, R. Kessinger, F. Cardullo and F. Diederich, *Helv. Chim. Acta*, 1997, **80**, 2238; (*h*) K. M. Kadish, X. Gao, E. V. Caemelbecke, T. Hirasaka, T. Suenobu and S. Fukuzumi, *J. Phys. Chem. A*, 1998, **102**, 3898.

2 (*a*) Y. Wang, *Nature*, 1992, **356**, 585; (*b*) K. C. Hwang and D. Mauzerall, *J. Am. Chem. Soc.*, 1992, **114**, 9705; (*c*) K. C. Hwang and D. Mauzerall, *Nature*, 1993, **361**, 138; (*d*) Y. Wang, R. West and C-H. Yuan, *J. Am. Chem. Soc.*, 1993, **115**, 3844; (*e*) C. P. Luo, C. H. Huang, L. B. Gan, D. J. Zhou, W. S. Xia, Q. K. Zhuang, Y. Zhao and Y. Y. Huang, *J. Phys. Chem.*, 1996, **100**, 16685.

3 (*a*) R. C. Haddon, *Nature*, 1991, **350**, 320; (*b*) A. F. Hebard, M. J. Rosseinsky, R. C. Haddon, D. W. Murphy, S. H. Glarum, T. T. M. Palstra, A. P. Ramirez and A. R. Kortan, *Nature*, 1991, **350**, 600; (*c*) K. Tanigaki, T. W. Ebbesen, J. Sato, J. Mizuki, J. S. Tsai, Y. Kubo and S. Kuroshima, *Nature*, 1991, **352**, 222; (*d*) P. J. Benning, D. M. Poirier, T. R. Ohno, Y. Chen, M. B. Jost, F. Stepniak, G. H. Kroll, J. H. Weaver, J. Fure and R. E. Smalley, *Phys. Rev. B*, 1992, **45**, 6899.

4 (*a*) P-K. Allemand, K. C. Khemani, A. Koch, F. Eudl, K. Holczer, S. Donovan, G. Gruner and J. D. Thompson, *Science*, 1991, **253**, 301; (*b*) K. Tanaka, A. A. Zakhidov, K. Yoshizawa, K. Okahara, T. Yamabe, K. Yasuki, K. Kikuchi, S. Sizuki, I. Ikemoto and Y. Achiba, *Phys. Lett. A*, 1992, **164**, 354; (*c*) V. Buntar, F. M. Sauerzopf and H. W. Weber, *Aust. J. Phys.*, 1997, **50**, 329; (*d*) S. Hino, K. Umishima, K. Iwasaki, K. Tanaka, T. Sato, T. Yamabe, K. Yoshizawa and K. Okahara, *J. Phys. Chem. A*, 1997, **101**, 4346.

5 (*a*) S. H. Friedman, D. L. DeCamp, R. P. Sijbesma, G. Srdanov, F. Wudl and G. L. Kenyon, *J. Am. Chem. Soc.*, 1993, **115**, 6506; (*b*) R. Sijbesma, G. Srdanov, F. Wudl, J. A. Castoro, C. Wilkins, S. H. Friedman, D. L. De Camp and G. L. Kenyon, *J. Am. Chem. Soc.*, 1993, **115**, 6510; (*c*) A. S. Boutorine, H. Tokuyama, M. Takasugi, H. Isobe, N. Nakamura and C. Helene, *Angew. Chem.*, 1994, **23**, 2526; (*d*) A. Hirsch, *The Chemistry of the Fullerenes*, Thieme Medical Publishers Inc., New York, 1994.

6 (*a*) M. Prato, T. Suzuki, F. Wudl, V. Lucchini and M. Maggini, *J. Am. Chem. Soc.*, 1993, **115**, 7876; (*b*) M. S. Meier, M. Poplawska and A. L. Compton, *J. Am. Chem. Soc.*, 1994, **116**, 7044; (*c*) T. Suzuki, Y. Maruyama, T. Akasaka, W. Ando, K. Kobayashi and S. Nagase, *J. Am. Chem. Soc.*, 1994, **116**, 1359; (*d*) N. Martin, L. Sanchez, B. Illescas and I. Perez, *Chem. Rev.*, 1998, **98**, 2527.

7 (*a*) R. M. Williams, J. M. Zwier and J. W. Verhoeven, *J. Am. Chem. Soc.*, 1995, **117**, 4093; (*b*) K. G. Thomas, V. Biju, M. V. George, D. M. Guldi and P. V. Kamat, *J. Phys. Chem. A*, 1998, **102**, 5341.

8 D. M. Guldi, M. Maggini, G. Scorrano and M. Prato, *J. Am. Chem. Soc.*, 1997, **119**, 974.

9 (*a*) D. Kuciavskas, S. Lin, G. R. Seely, A. L. Moore, T. A. Moore, D. Gust, T. Drovetskaya, C. A. Reed and P. D. W. Boyd, *J. Phys. Chem.*, 1996, **100**, 1592; (*b*) H. Imahori, K. Hagiwara, M. Aoki, T. Akiyama, S. Taniguchi, T. Okada, M. Shirakawa and Y. Sakata, *J. Am. Chem. Soc.*, 1996, **118**, 11771.

10 (*a*) P. A. Liddell, D. Kuciauskas, J. P. Sumida, B. Nash, D. Nguyen, A. L. Moore, T. A. Moore and D. Gust, *J. Am. Chem. Soc.*, 1997, **119**, 1400; (*b*) H. Imahori, S. Cardoso, D. Tatman, S. Lin, L. Noss, G. R. Seely, L. Sereno, J. Chessa de Silber, T. A. Moore, A. L. Moore and D. Gust, *Photochem. Photobiol.*, 1995, **62**, 1009.

11 (*a*) D. M. Guldi, H. Hungerühler and K-D. Asmus, *J. Phys. Chem.*, 1995, **99**, 13487; (*b*) B. Ma, E. C. Bunker, R. Guduru, X. Zhang and Y-P. Sun, *J. Phys. Chem. A*, 1997, **101**, 5626; (*c*) D. K. Palit, H. Mohan, P. R. Birkett and J. P. Mittal, *J. Phys. Chem. A*, 1997, **101**, 5418; (*d*) C. Luo, M. Fujitsuka, C-H. Huang and O. Ito, *J. Phys. Chem. A*, 1998, **102**, 8716.

12 (*a*) D. M. Guldi, H. Hungerühler and K-D. Asmus, *J. Phys. Chem.*, 1995, **99**, 9380; (*b*) D. M. Guldi and K-D. Asmus, *J. Phys. Chem. A*, 1997, **101**, 1472.

13 (*a*) N. Wiberg, *Angew. Chem., Int. Ed. Engl.*, 1968, **7**, 766; (*b*) K. Kuwata and D. Geske, *J. Am. Chem. Soc.*, 1964, **86**, 2101.

14 M. Fujitsuka, C. Luo and O. Ito, *J. Phys. Chem. B*, 1999, **103**, 445.

15 A. Watanabe and O. Ito, *J. Phys. Chem.*, 1994, **98**, 7736.

16 (*a*) G. A. Heath, J. E. McGrady and R. L. Martin, *J. Chem. Soc., Chem. Commun.*, 1992, 1272; (*b*) R. D. Bolskar, S. H. Gallagher, R. S. Armstrong, P. A. Lay and C. A. Reed, *Chem. Phys. Lett.*, 1995, **247**, 57.

17 P. C. Trulove, R. T. Carlin, G. R. Eaton and S. S. Eaton, in *Fullerene*, ed. R. S. Ruoff and K. M. Kadish, Electrochemical Society, Pennington, NJ, 1995, p. 362.

18 C. Luo, M. Fujitsuka, A. Watanabe, O. Ito, L. Gan, Y. Huang and C-H. Huang, *J. Chem. Soc., Faraday Trans.*, 1998, **94**, 527.

19 H. A. Benesi and H. A. Hildebrand, *J. Am. Chem. Soc.*, 1949, **71**, 2703.

20 (*a*) P. Scharff and N. Feldtner, *Mol. Phys. Rep.*, 1997, **18/19**, 137; (*b*) V. Brezova, A. Stasko, P. Rapta, D. M. Guldi, K-D. Asmus and K-P. Dinse, *Magn. Reson. Chem.*, 1997, **35**, 795.

21 P. R. Wells, *Linear Free Energy Relationship*, Academic Press Inc., New York, 1968.

22 D. Rehm and A. Weller, *Isr. J. Chem.*, 1970, **8**, 259.

Paper 9/01837I